Chemistry–A European Journal
Concept
doi.org/10.1002/chem.202402566
Chemistry Europe
European Chemical Societies Publishing
www.chemeurj.org

Recent Advances in DNA-Based Nanoprobes for *In vivo* MiRNA Imaging

Caixia Wang,[a] Xuefang Song,[a] Jieyu Shen,[a] Yuxin Xie,[a] Huangxian Ju,[a] and Ying Liu*[a, b]

As a post transcriptional regulator of gene expression, microRNAs (miRNA) is closely related to many major human diseases, especially cancer. Therefore, its precise detection is very important for disease diagnosis and treatment. With the advancement of fluorescent dye and imaging technology, the focus has shifted from *in vitro* miRNA detection to *in vivo* miRNA imaging. This concept review summarizes signal amplification strategies including DNAzyme catalytic reaction, hybrid chain reaction (HCR), catalytic hairpin assembly (CHA) to enhance detection signal of lowly expressed miRNAs; external stimuli of ultraviolet (UV) light or near-infrared region (NIR) light, and internal stimuli such as adenosine triphosphate (ATP), glutathione (GSH), protease and cell membrane protein to prevent nonspecific activation for the avoidance of false positive signal; and the development of fluorescent probes with emission in NIR for *in vivo* miRNA imaging; as well as rare earth nanoparticle based the second near-infrared window (NIR-II) nanoprobes with excellent tissue penetration and depth for *in vivo* miRNA imaging. The concept review also indicated current challenges for *in vivo* miRNA imaging including the dynamic monitoring of miRNA expression change and simultaneous in vivo imaging of multiple miRNAs.

Introduction

MicroRNAs (miRNAs) are a class of short single-stranded endogenous non-coding RNA molecules with a length of 21–23 nucleotides.[1] The biogenesis of miRNAs involves multiple steps, starting from the transcription of miRNA genes to generate primary miRNA (pri-miRNA).[2] Pri-miRNA is processed by the Drosha enzyme in the cell nucleus to produce precursor miRNA (pre-miRNA), which is then transported to the cytoplasm and further processed by the Dicer enzyme to form mature double-stranded miRNA (ds-miRNAs).[3] The final step involves the unwinding of ds-miRNAs to release the mature single-stranded miRNA.[4] MiRNAs play a crucial role in the regulation of gene expression, particularly in the regulation of messenger RNA (mRNA) expression. By binding to complementary target mRNAs, miRNAs post-transcriptionally regulate gene expression, leading to mRNA degradation and inhibition of mRNA translation.[5] Through this mechanism, miRNAs participate in the regulation of various physiological processes such as cell development, differentiation, proliferation, apoptosis, hematopoiesis, as well as immune development and response.[4] MiRNA-124 enhances neural development and is overexpressed in mature neurons.[6] MiRNA-296 expression level decreases during stem cell differentiation process, while miRNA-21 and miRNA-22 expression levels increase during the progression process.[7] MiRNA-155 is usually upregulated following B cell activation.[8]

Clinical evidence are emerging which suggest that the abnormal expression of miRNAs are closely related to many serious human diseases, For example, miRNA-21 is upregulated in breast cancer patients, and is associated with tumor progression;[9] miRNA-132, miRNA-185 are upregulated in gastric cancer patients;[10] and miRNA-196, miRNA-106 are overexpressed in cancer metastatic stages.[11] These make miRNA potential diagnostic biomarkers with clinical application prospect for early cancer detections[12] and treatments. Therefore, obtaining quantitative information on miRNA expression is crucial for understanding miRNA-related physiological and pathological processes, diagnosing miRNA-related diseases, and developing miRNA-based therapeutic approaches.[13] Due to the stable release of miRNA in body fluids, liquid biopsy has become an important non-invasive diagnostic method for circulating miRNA.[14] However, liquid biopsy faces challenges such as complex sample processing process and strong background interference from body fluid components. In addition, the concentration of miRNAs were diluted by body fluids and lost spatial localization information once released into systemic circulation.[15] In addition to *in vitro* miRNAs detection, *in vivo* imaging the location and expression level of miRNAs is also important. Due to the short length, low abundance, sequence homology of miRNAs,[16] as well as the complexity of the in vivo physiological environment, precise imaging of miRNAs *in vivo* still faces major challenges: (1) low abundance miRNA in live cells, (2) dynamic changes in miRNA expression levels in the physiological environment, (3) nonspecific responses of nanoprobes during delivery in the complex physiological environment, and (4) high background signals from spontaneous fluorescence in live tissue. Therefore, it is crucial to develop appropriate nanoprobes with good detection sensitivity and selectivity for precise miRNA imaging.

DNA is not only the carrier of genetic information, but also the base unit for construction of bio-nanomaterials. It has

[a] C. Wang, X. Song, J. Shen, Y. Xie, H. Ju, Y. Liu
State Key Laboratory of Analytical Chemistry for Life Science, School of Chemistry and Chemical Engineering, Nanjing University, Nanjing 210023, P. R. China
E-mail: yingliu@nju.edu.cn
[b] Y. Liu
Chemistry and Biomedicine Innovation Center, Nanjing University, Nanjing 210023, P. R. China

excellent biocompatibility and ease of functionalization modification.[17] Through phosphorothioate modification of DNA backbones,[18] self-assembling to rigid structures,[19] and conjugating with nanomaterials,[20] stability of DNA nanostructures could be enhanced which efficiently prevent them from nuclease degradation. Due to the highly specific and programmable nature of DNA based nanostructures, their applications in materials science and biology are growing explosively.[21] Currently, an increasing amount of research is focusing on designing DNA nanoprobes to identify target molecules and convert recognition events to readable signal outputs. In particular, significant efforts have led to the design of DNA-based nanostructures for detecting and imaging a wide range of analytes, including metal ions, small molecules, RNA, and proteins,[22] which show great potential in revealing the fundamental mechanisms of pathophysiological processes at the molecular level and promoting disease diagnosis. DNA nanoprobes could also be conveniently assembled with gold nanoparticles, iron nanoparticles, and various fluorescent molecules, which obtain corresponding surface-enhanced Raman scattering (SERS),[23] photoacoustic imaging (PAI)[24] and magnetic resonance imaging (MRI)[25] signal change in response to target molecules, such as miRNAs.

In this concept, we summarize the recent progress on the application of functional DNA nanoprobes for *in vivo* miRNA imaging. As shown in Scheme 1, DNA nanoprobes can be integrated with nucleic acid cascade reactions for signal amplification, incorporated with competitive binding strand, pH responsive strand, and light responsive strand for regulating and monitoring dynamic hybridization/dehybridization events, combined with DNA logical operation strands to prevent false positive signals, and conjugated with the second near-infrared window (NIR-II) materials for *in vivo* bioimaging. This concept highlights the design of signal amplification strategies for intracellular and *in vivo* miRNA imaging, discusses DNA calculation strategies for avoidance nonspecific miRNA signal, introduces NIR-II nanoprobes for in vivo miRNA imaging, as well as prospects current challenges and future opportunities in this emerging field.

DNA Signal Amplification Strategies for Low Abundance miRNA Detection

Fluorescent nanoprobes can be utilized for real-time monitoring target concentration changes at local environments.[26] However, traditional fluorescent nanoprobes are designed with a 1:1 signal output to input ratio, which is not sufficiently sensitive for detecting low abundance targets in biologyical environments.[27] Given the minimal miRNA content in living cells (miRNA comprising only 0.01% of total RNA mass),[4]

Caixia Wang obtained her bachelor degree from Hubei Normal University in 2017, and mater degree from Southwest University in 2020. She is currently pursuing her Ph.D. degree under the guidance of Prof. Ying Liu in Nanjing University. Her research focuses on the design of DNA functionalized rare earth nanoprobes and their application in cancer diagnosis and therapy.

Xuefang Song obtained her bachelor degree from Dalian University of Technology in 2022, and is currently pursuing her master degree under the guidance of Prof. Ying Liu in Nanjing University. Her research focuses on the design and synthesis of NIR-II fluorescence probes for cancer subtype discrimination.

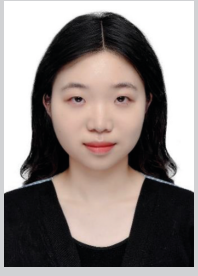

Jieyu Shen obtained her bachelor degree from Jilin University in 2022, and is currently pursuing her master degree under the guidance of Prof. Ying Liu in Nanjing University. Her research focuses on the design of DNA nanoprobes and their application in cell surface engineering and cancer immunotherapy.

Ying Liu is currently a professor at Nanjing University, China. She obtained her bachelor degree in 2004 and master degree in 2007 from Nanjing University, and Ph.D. degree in 2012 from University of California, Riverside. After completed postdoc training in University of California, Davis, she joined Nanjing University as an overseas high-level talent in 2015. She won the fund support of Chinese National Excellent Young Scholars in 2020. Her research interest focuses on the development of responsive nanomaterials for bioimaging and therapy.

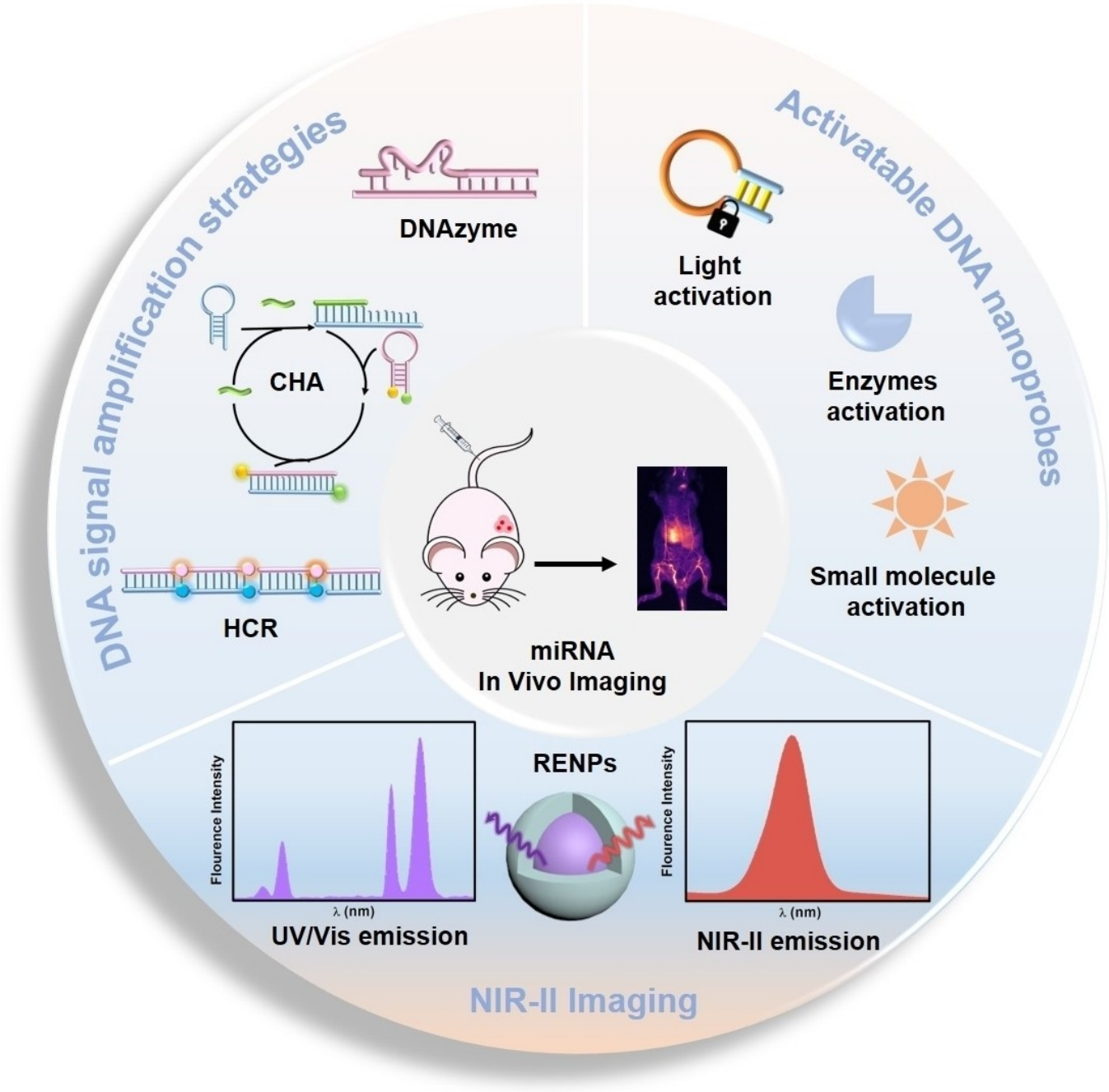

Scheme 1. Schematic illustration of the application of DNA signal amplification strategies, activatable DNA probes, and rare earth nanoparticles (RENPs) for in vivo miRNA imaging.

various signal amplification techniques such as entropy-driven catalyst DNAzyme,[28] hybrid chain reaction (HCR),[29] catalytic hairpin assembly (CHA),[30] rolling circle amplification (RCA),[31] and strand displacement amplification (SDA)[32] are employed as signal amplification strategies to achieve high detection sensitivity.

DNAzyme Signal Amplification

DNAzymes are catalytic nucleic acids,[33] which have been widely applied for signal amplification of nucleic acids targets due to their good heat and chemical stability, as well as easy synthesis and modification processes.[34] DNAzyme based catalytic reaction was successfully developed for metal ions detection in homogeneous solution.[35] The enzyme-activatable DNAzyme sensor (E-DZM) was established by incorporating DNAzyme with an abasic (AP) site for cancer cell specific Zn^{2+}

detection. E-DZM was delivered into cell with its substrate strands, where human apurinic/apyrimidinic endonuclease 1 (APE1) recognized AP site, activated DNAzyme to cleave substrate strands in presence of Zn^{2+} with fluorescence recovery. Though efficiently amplified detection signal, DNAzyme cascade reactions that proceeds in homogeneous reaction environment impairs reaction efficiency and requires long reaction time. Confining continuous DNA reactants in a compact space can maintain high local reagent concentrations, promote substrate transport, protect them from damage, and accelerate reactions. Li et al. reported a DNAzyme driven DNA walker for intracellular miRNA detection.[36] The nano-system was constructed on gold nanoparticle (AuNP) decorated with hundreds of substrate strands serving as DNA tracks and dozens of DNA walker strand that modified with DNAzyme at its terminus. DNAzyme was silenced by a locking strand. The intracellular target miRNA released locking strand, activated DNAzyme and initiated its continuous cleavage of DNA tracks with fluorescence recovery, which enabled amplified detection signal of target miRNA in cancer cells (Figure 1a). The signal amplification effect and specific activation was confirmed by intracellular confocal laser scanning microscope imaging (Figure 1b). The DNAzyme-imaging machinery shows substantially high amplification gain without signal leakage, which was especially promising for in situ amplified detection of trace amount of analytes. Additionally, DNAzyme can perform synergistic functions: as a signal amplifier for visualizing low-abundance biomarkers and as a therapeutic tool for miRNA responsive treatment activation. Liu et al. reported a miRNA-responsive multifunctional nanocabinets (MFNCs) that utilize DNAzyme catalyzed cascade reactions for both Cy5 fluorescence recovery to visualize miRNA and DOX release for breast cancer therapy.[37]

Catalytic Hairpin Assembly (CHA)

CHA doesn't require enzyme participation in reaction process,[14] which is more appropriate wider application environments. In a typical CHA system, the initiator strand, usually the target miRNA, catalyzes the assembly of nucleic acid hairpins into biphasic products via continuous hybridization process driven by isothermal free energy.[38] The nucleic acid target triggers the opening of a first hairpin by hybridizing in the stem region. The target is then displaced by the binding of a second hairpin, and is thus recycled in the process.

The cycling characteristics of CHA initiators make it particularly suitable for amplification analysis of low abundance biomarkers of clinical importance.[39] Liu et al.[40] reported a miRNA-triggered CHA reaction for low-abundance miRNA detection. The nanosystem consists of capture probe H1 modified with Cy5 which is immobilized on AuNPs, and catalytic probe H2 modified with Cy3/BHQ. Target miRNA hybridizes with H1, initiating a branch migration reaction to recover Cy5

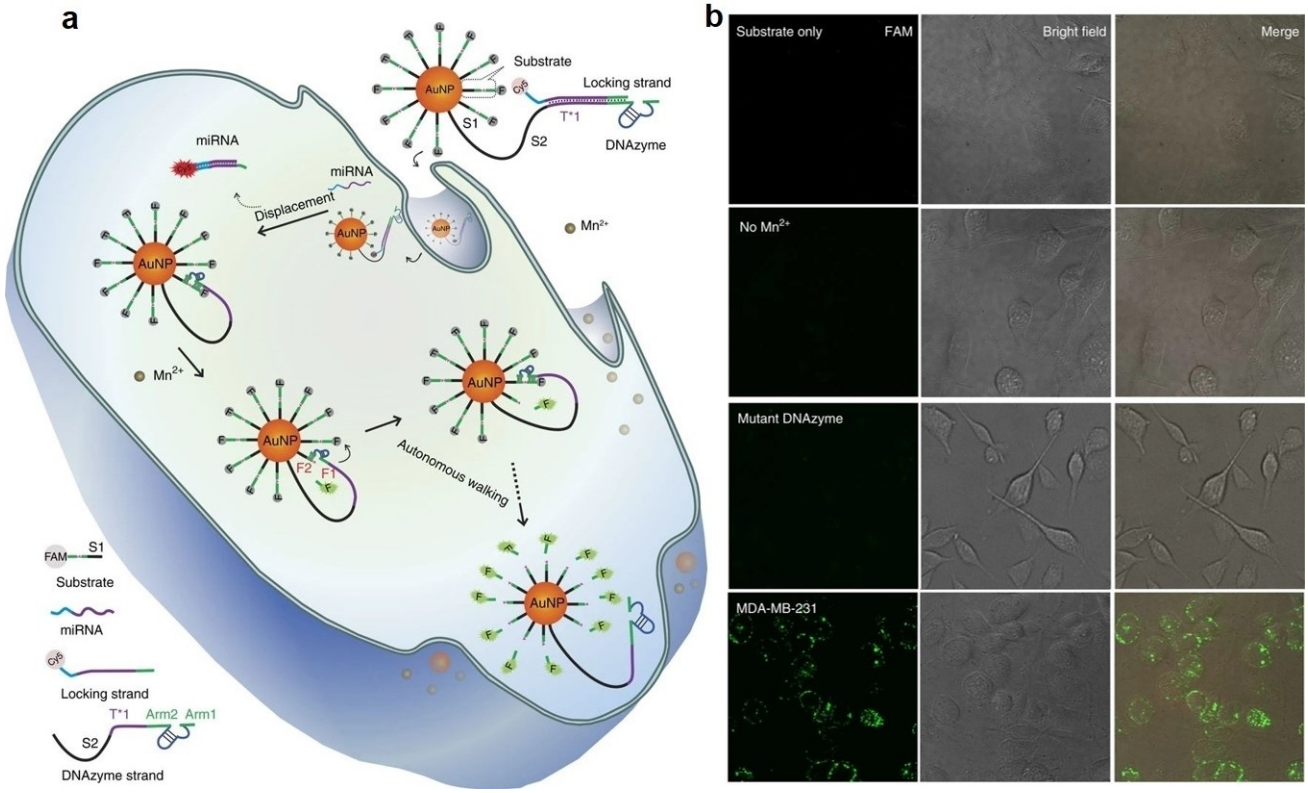

Figure 1. a) Schematic of DNAzyme motor operation initiated by intracellular miRNA. b) Confocal fluorescence imaging of MDA-MB-231 cells treated with DNAzyme system, and control groups that only treated with DNAzyme substrate, in the absence of Mn^{2+}, treated with a mutant DNAzyme motor system and Mn^{2+}. Reproduced from Ref.[36] with permission. Copyright 2016 Springer Nature.

fluorescence and exposing the hybridization zone for H2 (Figure 2a, Step b). Hybridization of H2 recovered Cy3 fluorescence and released target miRNA for next round of H1/H2 assembly on AuNPs (Figure 2a, Stpe c–e). The signal amplification effect and dual-color fluorescent recovery were confirmed by intracellular confocal laser scanning microscopy imaging (Figure 2b). Similar strategies were also developed for three-dimensional (3D) high-resolution profiling of key miRNA molecules in migrating cells.[41]

Hybridization Chain Reaction (HCR)

HCR appears as an autonomous DNA hybridization process, which produces a long, notched, tandem, double stranded DNA nanowire through the cross opening of DNA hairpins.[42] HCR has a high signal amplification ability while maintaining a low background.[43] Wu and coworkers[44] developed a novel fluorescent probe that for the first time enabled RNA imaging in living mice via an *in vivo* HCR using a cell-targeting tripartite DNA probe which constructed by assembling three DNA motifs to form a Y-shaped probe via sticky-end hybridization. One motif is a cell targeting DNA-peptide (poly-lysine) conjugated folate probe (FAP) and the other two motifs are hairpin probes H1 and H2, which undergo HCR assembly in response to a target RNA. When systemically administered into a living mouse via intravenous injection, the tripartite DNA probe can be selectively taken up into tumor cells. The presence of target RNA mediates a cascade of alternating assembly between probes H1 and H2 via the HCR circuit, generating an activated NIR fluorescence response for in vivo RNA imaging in the living mouse. The realization of an *in vivo* HCR signal amplification strategy allowed visualization of low-abundance RNAs in living animals. Wang et al. also constructed an autocatalytic DNAzyme (ACD) bio-circuit for amplified miRNA imaging *in vivo* by coupling HCR and DNAzyme biocatalytic reaction sustained by a honeycomb MnO_2 nanosponge (hMNS)s,[26] which served as a precursor of the DNAzyme cofactor for facilitating intracellular DNAzyme biocatalysis. MiRNA-21 initiated HCR for autonomous assembly of DNAzyme nanowires, while endogenous GSH released Mn^{2+} from hMNSs to act as cofactor of DNAzyme.

However, the kinetics of HCR and CHA depends on the diffusion of DNA reactants for random collision and interaction in the homogeneous environment.[45] The reaction proceeding requires continuously searching for the next hybridizing probe in a three-dimensional fluidic space, which greatly prolongs the reaction time and compromises the reaction efficiency. Confining successive reactants together in a compact space maintains high local concentrations of reagents and thus promotes substrate transportation, protects them against damage, and accelerates reactions.[46] DNA self-assembled nanocages[47] and cell membrane were used as confined reaction areas, which effectively accelerated enzymatic reactions.[48] We designed a DNA "nano string light" (DNSL) as confined reaction area to perform DNA cascade reaction (DCR) for efficient target mRNA imaging in living cells[49] (Figure 3a). DNSL was constructed by interval hybridization of modified DNA hairpin probe pairs (H1 and H2) to a DNA nanowire produced via RCA reaction. Target mRNA initiated HCR, which was accelerated via domino effect on DNA nanowire. The confined area effectively enhanced local concentration of H1/H2 and enhanced reaction rate about 6.7 times to shorten over 2 hours reaction in 20 minutes (Figure 3b,c). In addition, we extended the application of accelerated HCR to multiplex detection with a photonic crystal (PC) array, which not only spatially distinguished different miRNA targets, but also further amplified miRNA detection signals.[50] The confined area accelerated HCR was also coupled with upconversion nanoparticle (UCNPs),[51] DNA polymers[52] for miRNA detections. We designed a photo-caged DNA nanocomb for preparation of NIR photo-switched cascade reaction triggered by specific microRNA and precise PDT of early-stage cancers (Figure 3d). This amplifier was composed of photo-caged DNA nanocombs and UCNPs with multiple upconversion luminances. The photozipper could be cleaved under NIR light to expose a sequence complementary with miRNA-21 for triggering the miRNA-responsive cascade hybridization reaction between H1 and H2, which activated the PPa' molecules arrayed in photo-caged DNA nanocomb for enhanced PDT. The photozipper was cleaved upon 808 nm laser radiation to expose miRNA recognition region, which induced subsequent cascade hybridization reaction upon miRNA-21 recognition to recover Cy3 fluorescence (Figure 3e,f). The recovered Cy3 fluorescence intensity reached the maximum value with NIR radiation for

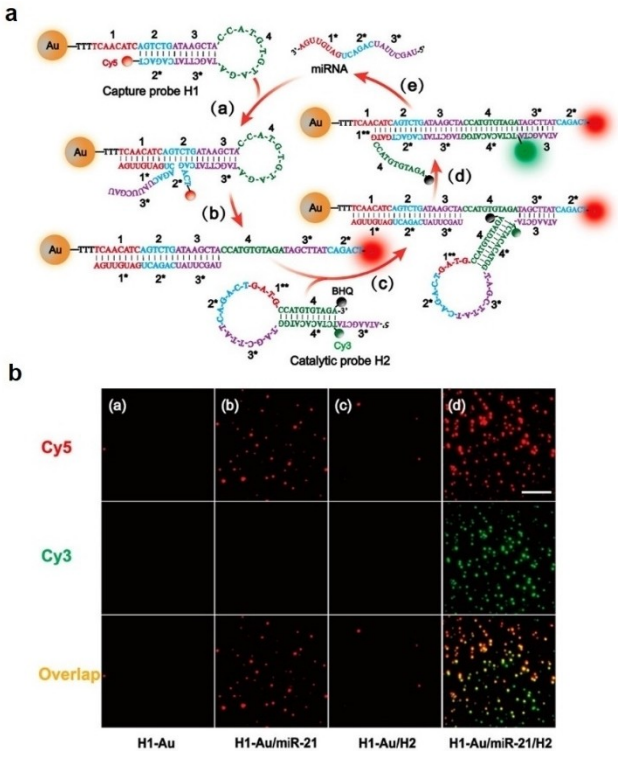

Figure 2. a) Structure and design of miRNA triggered CHA reaction for signal amplification b) Fluorescence imaging of H1 modified AuNPs (H1-Au) (a); H1-Au NPs with miR-21 (H1-Au/miR-21) (b); H1-Au NPs with H2 (H1-Au/H2) (c); H1-Au NPs with miR-21 and H2 (H1-Au/miR-21/H2) (d). Reproduced from Ref.[40] with permission. Copyright 2020 American Chemical Society.

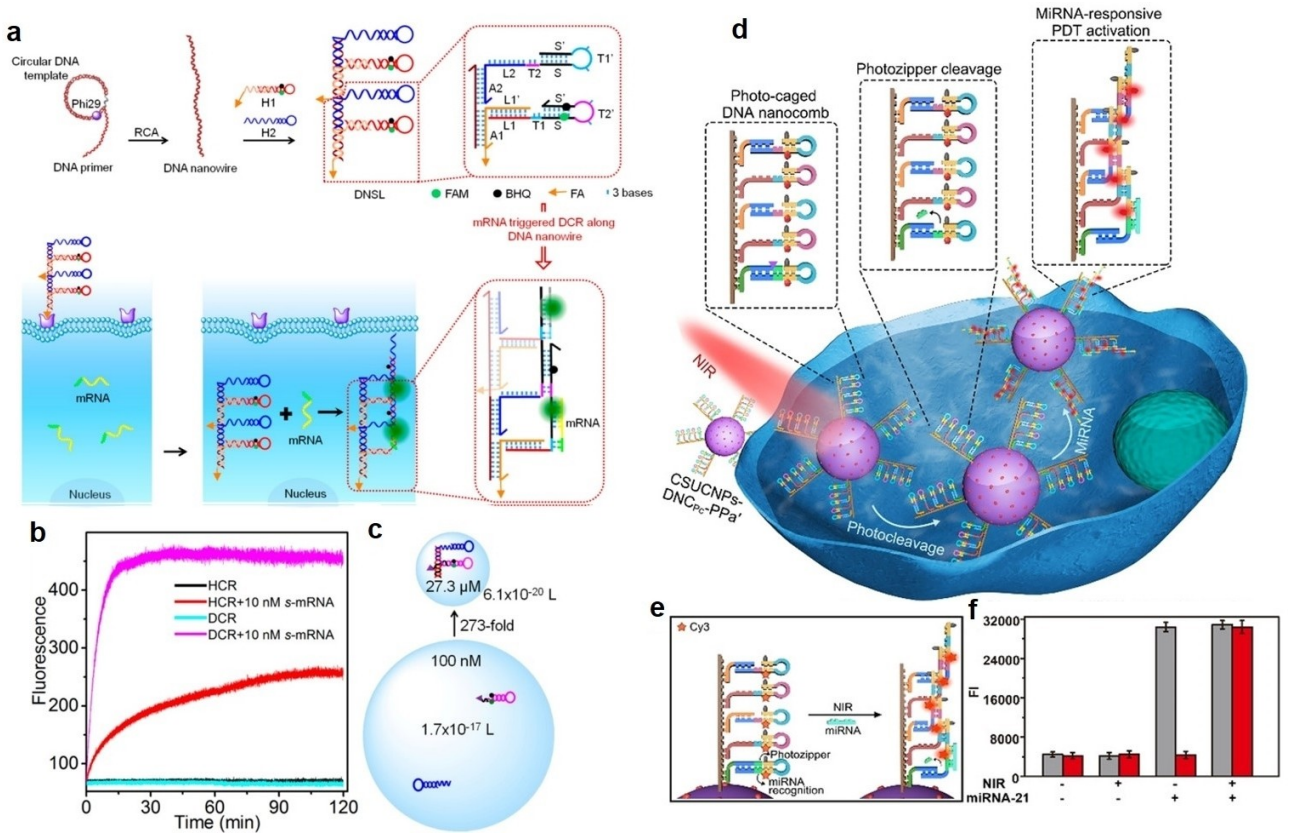

Figure 3. a) Schematic illustration of DNSL synthesis based on interval hybridization of H1 and H2 to a DNA nanowire and targeted delivery of DNSL and imaging of target mRNA in living cells based on accelerated DCR along DNA nanowire. b) Time-dependent fluorescence spectra of DCR in 100 nM DNSL and HCR in a homogeneous solution containing 100 nM H1 and 100 nM H2 in response to 10 nM survivin mRNA (smRNA). c) Comparison of the reaction area and local concentration of H1 and H2 for DCR and HCR. Reproduced from Ref.[49] with permission. Copyright 2018 American Chemical Society. Schematic illustrations of d) NIR photo-switched miRNA amplifier for precise PDT and e) NIR-induced photozipper cleavage and miRNA-responsive cascade hybridization reaction on CSUCNPs-DNCPc–Cy3 and f) corresponding fluorescence recovery in presence/absence of NIR irradiation and miRNA-21. Reproduced from Ref.[51] with permission. Copyright 2020 Wiley-VCH Verlag GmbH & Co. KGaA, Weinheim.

30 min due to the increased local concentration of hairpins and thus accelerated the DNA cascade reaction.

Activatable DNA Nanoprobes for miRNA Imaging

Traditional DNA fluorescent nanoprobes adopt an "always active" design, which rely on tumor accumulation of nanoprobes to light up the tumor position. However, this "always active" DNA nanoprobe is vulnerable to the tumor microenvironment in the systemic circulation or extracellular target miRNAs in serum, resulting in non-specific fluorescence signal recovery outside the cells, leading to false positive signals.[53] To avoid non-specific responses of the "always active" DNA nanosensor during delivery, researchers have developed "active" nanoprobes where the probes remain in "off" state in the absence of stimuli and couldn't recognize targets, and become active with recovered recognition capability of detection targets. The stimuli include external stimuli including light, ultrasound, and internal stimuli including enzyme and small molecules.

DNA Nanoprobes with External Stimuli

Due to its high spatiotemporal controllability, light is often used as an external stimulus for various specific activation of nanomachine switches to enhance precision of target imaging. The Deiters et al. developed a ultraviolet (UV) light activated DNA logic gate for intracellular miRNA imaging.[54] UV irradiation disrupted the "light cage" at specific time points and initiated a chain displacement reaction to produce signal output. Subsequently, Lu et al. designed a UV light activated DNAzyme for highly specific imaging of intracellular Zn^{2+}.[55] In this design, the adenosine ribonucleotide was replaced by 2′-O-nitrobenzyl adenosine, which avoided DNAzyme non specific activation during the delivery. UV irradiation disrupted 2′-O-nitrobenzyladenosine and promoted the recovery of deoxyribonuclease activity, thereby achieved intracellular Zn^{2+} specific imaging.

Despite the success of UV irradiation activatable nanoprobes, the high phototoxicity and limited tissue penetration

depth of UV irradiation restrict their *in vivo* applications. Due to the enhanced tissue penetration capabilities and lower phototoxicity of near-infrared light, researchers have explored their possibilities as nanoprobes activation stimuli. Upconversion emission of rare earth nanoparticles (RENPs) convert NIR irradiation to UV emissions, therefore become an appropriate substitute for UV irradiation. Li et al. reported NIR-activated DNA nanodevices for the first time by utilizing UV upconversion emission of RENPs under NIR irradiation, and achieved specific *in vivo* ATP imaging.[56] The nanodevice not only enabled efficient intracellular delivery of nanoprobes, but also allowed the temporal control of nanoprobe activation via NIR irradiation. Zhao et al. also designed a NIR controlled activated DNA nanodevice by using upconversoin emission of RENPs, and achieved spatiotemporal controllable imaging of miRNAs in cells and mice.[57] A hairpin structured DNA probe was designed which contained a blocked miRNA recognition region and a photocleavable bond molecule (PC bond). Under NIR light irradiation, UCNPs acted as light conversion centers to convert NIR into UV light, and the emitted UV light cleaved the PC bond, and caused the closed hairpin chain to partially detach. After exposure to miRNA, the blocker strand released in accompany with fluorescence recovery (Figure 4a), thus successfully achieved spatiotemporal controllable miRNA imaging both intracellularly (Figure 4b) and in mice (Figure 4c,d). In order to avoid "false positive signal amplification" by extracellular analytes, we design a photo zipper locked miRNA responsive DNA nanomachine (PZ-DNA nanomachine) to protect the DNA nanomachine against nonspecific extracellular activation and allowed satisfactory signal amplification for sensitive miRNA imaging.[58] The-PZ-DNA nanomachine was composed of RENPs with surface functionalization of a target miRNA responsive DNA walker and its corresponding substrate DNA strands labelled with quencher BHQ2. Dye Cy3 was also co-immobilized on RENP surface to facilitate energy transfer from the interior RENP emission at 540 nm under NIR irradiation

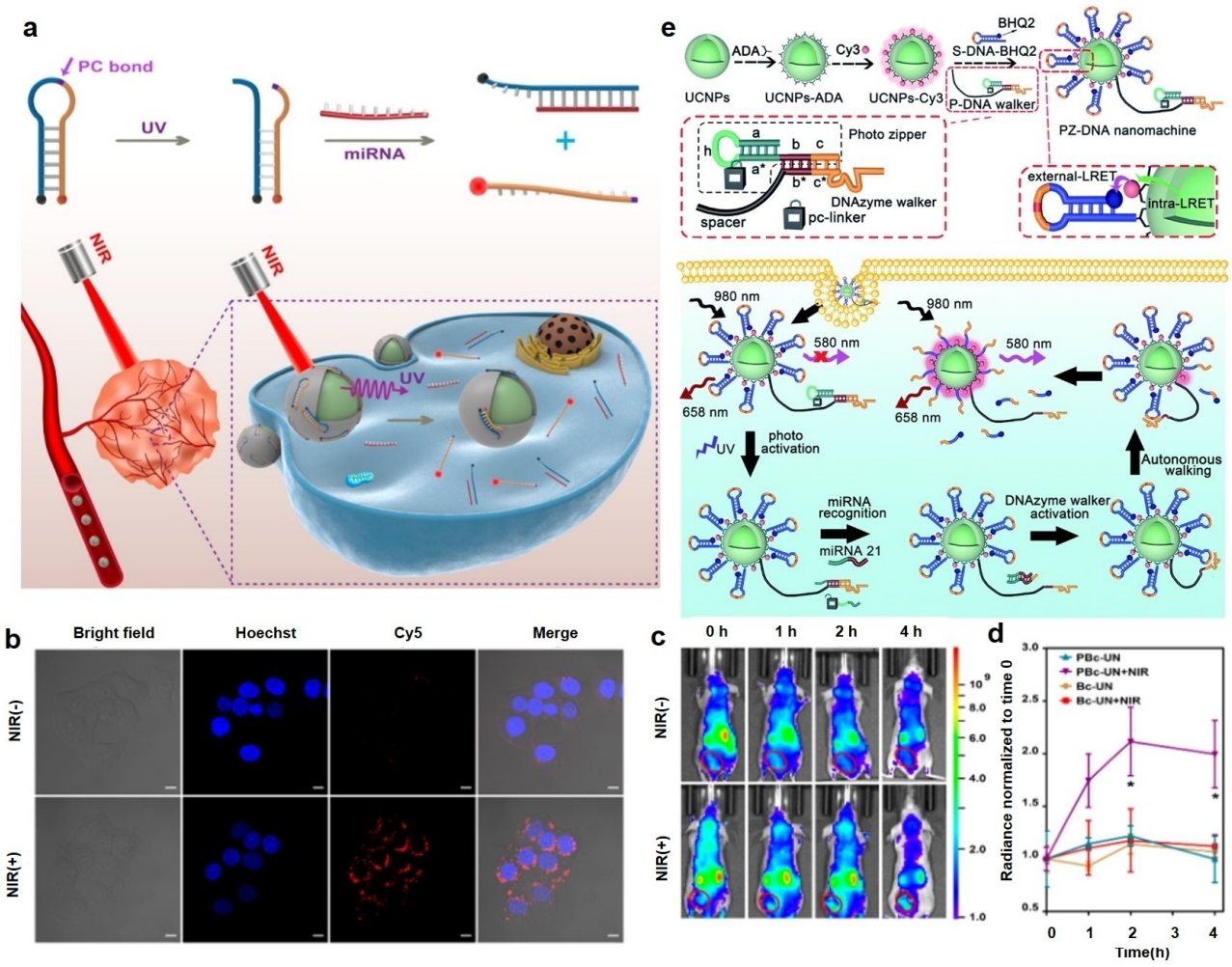

Figure 4. a) Schematic illustration of NIR irradiation-controlled miRNA imaging through the engineering of a photosensitive hairpin structured miRNA recognition probe which coupled with rare earth nanoparticle. b) Confocal fluorescence images of HeLa cells treated with photosensitive miRNA probe in the presence and absence of NIR irradiation. c) Fluorescence imaging of mice injected with photosensitive miRNA probe in the presence and absence of NIR irradiation at the tumor sites. d) The intratumoral fluorescence intensity of mice in (c). Reproduced from Ref.[57] with permission. Copyright 2019 American Chemical Society. e) Schematic illustrations of photo zipper locked DNA nanomachine and its operation in response to miRNA in living cells. Reproduced from Ref.[58] with permission. Copyright 2020 American Chemical Society.

to BHQ2 labelled at the terminus of the substrate DNA strands. After photo-activation, the PZ-DNA nanomachine was operated by intracellular miRNA and continuously cleaved the BHQ2 labelled substrate DNA strands, with corresponding Cy3 fluorescence recovery for intracellular miRNA imaging (Figure 4e). In conclusion, light serves as a satisfactory external stimulus with high spatiotemporal controllability for precise imaging of intracellular and *in vivo* targets.

DNA Nanoprobes with Internal Stimuli

Though NIR activation of nanoprobe provided satisfactory performance for mice subcutaneous tumor model. However, light illumination area usually lie in mm/cm size, which limits its resolution and hardly achieves precise imaging or regulation at cellular level.[59] Internal stimuli, such as tumor microenvironment highly expressed molecules, were also used for activatable nanoprobes. Compared with normal tissues, the expression of various small biomolecules (such as glutathione (GSH),[60] pH,[61] adenosine triphosphate (ATP)[56]) in tumor tissues is abnormally elevated, which serves as a common endogenous stimulus switch to design DNA nanomachines, thereby enhance the *in vivo* miRNA imaging specificity. Zhang et al. designed an endogenous ATP-driven DNA walker and successfully developed a ATP feuled DNA system for *in situ* spatiotemporal imaging of miRNAs in living cells.[62] A DNA walker system was coupled to gold nanoparticle which included a DNA walker strand and reactant DNA strands. The reactant DNA strands contain fluorescent dye, whose fluorescence was quenched by gold nanoparticles. The target miRNA activated DNA walker strand and released the fluorescent labelled DNA strand from gold nanoparticle to recover fluorescence. ATP, the small molecules that highly expressed in tumor microenvironment acted as the fuel strand to release fluorescent DNA strand from gold nanoparticle with enhanced fluorescence recovery. Chai et al. reported a GSH-activatable, aptamer-based DNA nanodevice sensor combined with nanoparticle-based targeting capability to achieve a AND-gated controlled ATP and GSH imaging in mitochondria.[63] The DNA nanodevice was decorated with mitochondria-targeting molecules to achieve spatially differentiation of imaging signal. Self-quenched DNA nanodevice was consists of an ATP adapter and a block chain modified with disulfide bonds, which illuminated the probe in the presence of both GSH and ATP and achieved simultaneous imaging of GSH and ATP. This nanosystem can only be illuminated when encountered ATP and GSH simultaneously, enabling specific imaging of tumor tissue.

In addition to the small molecules that highly expressed in tumor microenvironment, enzymes also act as endogenous stimuli to activate nano-probes for specific biomaker imaging.[64] Many enzymes, including protease and DNA repair enzymes, are overexpressed in tumor cells, therefore become biomarkers of malignant tumors.[65] Li et al. reported a generalizable approach via the combination of enzymatically gated CHA (E-CHA) with lipid nanoparticles (LNPs)-based delivery strategy for tumor specific activation of signal amplification and sensitive miRNA imaging.[66] In this system, the enzyme-responsive molecular beacon (EMB) containing an abasic site was designed to prevent the target miRNA-induced conformational change of EMB and corresponding CHA reaction. Reaction with enzyme APE1 exposed target miRNA recognition position, which initiated CHA with strong fluorescence signal generation. In 2021, the Li group developed a protease-activated DNA nanomachine by introducing a peptide nucleic acid (PNA) to control the seal/exposure of ATP recognition region, and achieved precise ATP imaging in cells and mice.[64a] The ATP-aptamers were effectively shielded by PNA to prevent nonspecific activation. Upon entry into tumor cells, the overexpressed cathepsin B (CaB) cleaved the peptide, released the blocked sequence and recognized miRNA and resulted in intracellular fluorescence recovery (Figure 5a). Both confocal fluorescence image and flow cytometry confirmed the selective activation of nanoprobes by intracellular CaB protease for precise ATP imaging (Figure 5b–d).

In addition to intracellular small molecules and protease, membrane proteins/receptors that highly expressed on tumor cell membrane also act as specific stimuli to activate the DNA nanoprobes for miRNA recognition. We designed a transmembrane DNA logical computation strategy to activate a DNA nanomachine only in cancer cells from a complex solid tumor microenvironment[67] (Figure 5e). The DNA nanomachine was prepared by modifying DNA strands on UCNPs. LA-apt, a DNA strand anchoring to a cancer cell membrane overexpressed receptor, served as inputs 1. Hybridization with input 1 at the cell membrane to activate DNA nanomachine for intracellular miRNA-21 recognition, which served as inputs 2. The cascade hybridization with intracellular input 2 completed the "AND" gate operation and released a DNA strand L2 as output to operate the DNA nanomachine and correspondingly activated the photosensitizer for subsequent photodynamic therapy. Confocal fluorescence image demonstrated that only correct operation of input 1 (LA-apt) in the DNA logic gate ensures the following reaction with input 2 (miRNA-21), realizing activation of DNA nanomachine (Figure 5f,g). Incorrect DNA logic computation can trigger nonspecific activation and deactivation of DNA nanomachines (Figure 5f,h).

NIR-II Nanoprobe for *In Vivo* miRNA Imaging

Despite the success of signal amplification and nonspecific signal suppression strategies, most currently reported miRNA imaging probes has emission window located in visible (Vis) light region,[68] where biomolecules (flavins, lipofuscin, reticulin) would generate autofluorescence as background signal[69] and impaired the accuracy of *in vivo* application. However, miRNA imaging window has rarely extended to NIR-II (1000–1700 nm) region with deeper penetration, higher spatial resolution, lower photon scattering and background. RENPs generate multiple emissions with narrow bandwidths in a wide range from UV/Vis to NIR-II by adjusting rare-earth ions doping types and ratios.[70] This feature makes them appropriate materials for *in vivo* imaging.

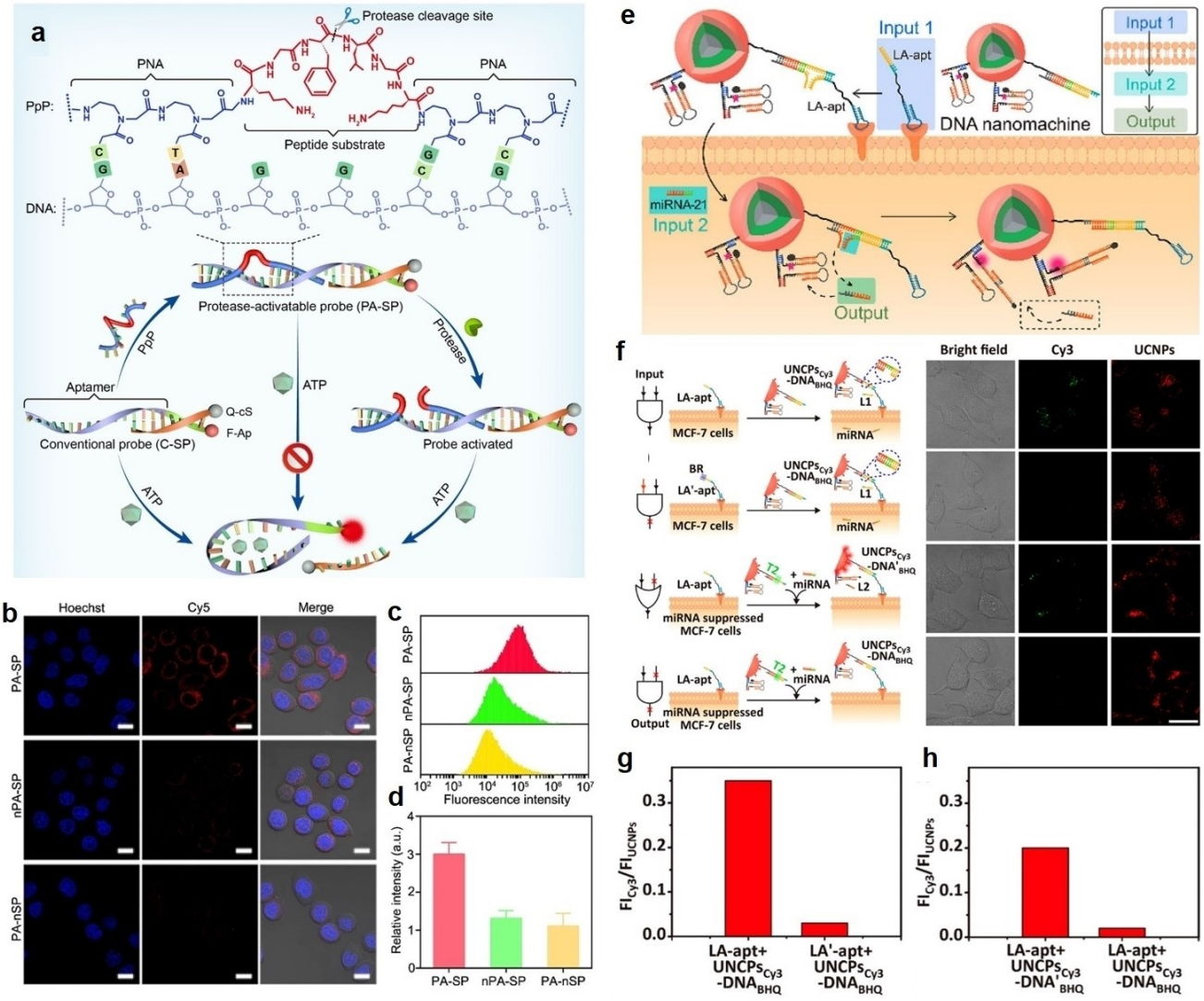

Figure 5. a) Schematic illustration of peptide nucleic acid (PNA) guided engineering of a DNA aptamer sensor for protease-activatable ATP detection. b) Confocal fluorescence images of HeLa cells treated with protease activatable aptamer probe (PA-SP), the control probes nPA-SP, which does not respond to protease, PA-nSP, which does not respond to ATP. Scale bars = 20 μm c, d) Flow cytometric quantification of intracellular fluorescence signal in (b). Reproduced from Ref.[64a] with permission. Copyright 2021 Wiley-VCH Verlag GmbH & Co. KGaA, Weinheim. (e) Structural diagram of the transmembrane DNA computation strategy (f) CLSM images of MCF-7 cells treated with LA-apt (a DNA strand recognized cancer cell membrane receptor) or LA′-apt (LA-apt with miRNA-21 blocking region) and then multishell UCNPs–Cy3-DNA-BHQ and (g) the corresponding intensity ratio of Cy3 fluorescence recovery over multishell UCNPs' luminance. CLSM images of miRNA-21 suppressed MCF-7 cells pretreated with LA-apt and incubated with miRNA-21-pretreated multishell UCNPs–Cy3-DNA-BHQ and multishell UCNPs–Cy3-DNA-BHQ and (h) its intensity ratio of Cy3 fluorescence recovery over multishell UCNPs' luminance. The scale bars indicate 25 μm. Reproduced from Ref.[67] with permission. Copyright 2020 American Chemical Society

Recently, we developed a NIR programmed *in vivo* miRNAs magnifier by conjugating activatable DNAzyme walker set to RENPs, which achieved effective NIR-II imaging of early stage tumor[71] (Figure 6a). Dye FD1080 (FD1080) modified substrate DNA quenched NIR-II downconversion emission of RENPs under 808 nm excitation. MiRNA recognition region in DNAzyme walker was sealed by a photo-cleavable strand to avoid "false positive" signal in systemic circulation. Upconversion emission of RENPs under 980 nm irradiation activated DNAzyme walker for miRNA recognition and amplified NIR-II fluorescence recovery of RENPs via DNAzyme catalytic reaction to achieve *in vivo* miRNA imaging. This study presented a novel approach for detecting low levels of biomarkers *in vivo* and diagnosing early-stage tumors. Tumor cell imaging indicated DNA nanomachine could realize activatable intracellular miRNA-21 imaging (Figure 6b, DNA nanomachine, NIR(+)), while showed little intracellular NIR-II fluorescence in the absence of 980 nm irradiation (Figure 6b, DNA nanomachine, NIR(−)) and "always active" DNA nanomachine (AA-DNA nanomachine) produced strong NIR-II fluorescence recovery from M-HeLa cells as "false positive" signal (Figure 6b, AA-DNA nanomachine, NIR(−)). This system successfully achieved accurate *in vivo* miRNA imaging (Figure 6c, DNA nanomachine, NIR(+)), while avoided nonspecific activation signal (Figure 6c, AA-DNA nanomachine, NIR(−)) and realized *in vivo* early tumor imaging (Figure 6d).

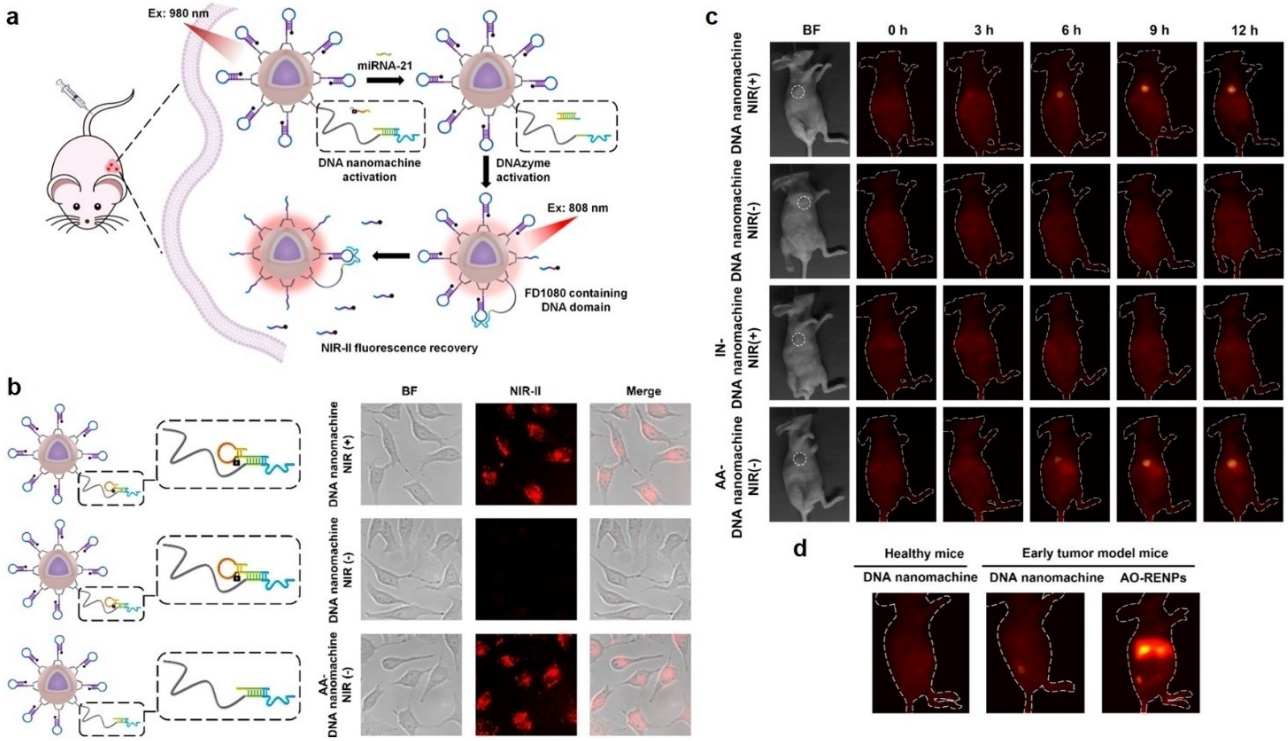

Figure 6. a) Schematic illustrations of NIR orthogonally programmed DNA nanomachine and *in vivo* NIR-II fluorescence recovery for miRNA-21 imaging, b) NIR-II fluorescence imaging of HeLa cells incubated with DNA nanomachine with or without 980 nm NIR irradiation, "always active" DNA nanomachine (AA-DNA nanomachine that doesn't have NIR response capability), *In vivo* NIR-II fluorescence imaging of c) tumor bearing mice in presence and absence of NIR irradiation, inactive DNA nanomachine (IN-DNA nanomachine that doesn't have miRNA responsive region) in presence of NIR irradiation, and AA-DNA nanomachine in absence of NIR irradiation, and d) healthy mice treated with DNA nanomachine and early tumor model mice treated with DNA nanomachine and "always on" imaging probe (AO-RENPs that does not respond to miRNA). Reproduced from Ref.[71] with permission. Copyright 2023 Wiley-VCH Verlag GmbH & Co. KGaA, Weinheim

Summary and Outlook

In this concept, we have reviewed the progress of functional DNA nanoprobes design and their applications in intracellular and *in vivo* miRNA imaging. Precise *in vivo* imaging of miRNAs faces significant challenges due to their short length, low abundance, sequence homology, and the complexity of the *in vivo* physiological environment. Therefore, various signal amplification strategies including DNAzyme reaction, HCR, CHA have been employed to amplify miRNA imaging signal. Stimuli-responsive DNA nanoprobes have also been developed with external stimulus such as NIR light and internal stimuli including tumor highly expressed small molecules such as ATP, GSH and enzymes such as APE1, CaB. With the advancement of imaging technology, the fluorescence detection region has shifted from visible region to NIR-II region with deeper tissue penetration depth and lower autofluorescence to improve the signal-to-noise ratio of *in vivo* imaging. Taking advantages of RENPs with programmable upconversion and downconversion emissions, *in vivo* miRNA imaging in NIR-II region has been reported.

Despite the progress made, there are issues that should be taken into consideration in future research of *in vivo* miRNA imaging. (1) miRNA expression are affected by many biological processes, which are keeping changing in live process. However, most currently reported nanoprobes all share the limitations of irreversible imaging signal, which can only trace the accumulation value of miRNA in the disease process, but cannot indicate the expression concentration decrease monitor the real-time concentration and spatiotemporal localization of miRNA in various dynamic equilibrium processes.[72] Therefore, dynamic visualization of both miRNA expression increase and decrease is important.[28] Reversible DNA structure transformation was successfully achieved via adding substitution chains to achieve dynamic miRNA detection.[73] Besides, state-adjustable fluorescent RNA (FLRNA) molecule was prepared which achieved dynamic analysis of miRNA concentration and its spatiotemporal localization in live cells.[72] More methodologies and strategies for dynamic monitoring miRNA expression change are expected. (2) Many physiological processes, as well as disease progression and therapy require the participation of multiple miRNAs. Cellular and in vivo multiple miRNAs imaging strategies have been reported via optically programming strand displacement reactions and developing combinational fluorescent dye bar-codes.[74] However, the emission probes are mainly organic dyes with wide detection windows located in visible region, which would lead to emission spectra overlap and in vivo intensity impairing due to tissue absorption and reflection. Multiple miRNA imaging in NIR-II region has not been achieved. Rare earth nanomaterials provide strong NIR-II emission with sharp band and programmable wavelength

regions, would become appropriate probe material for in vivo multiple miRNAs imaging.

Acknowledgements

We gratefully acknowledge the National Natural Science Foundation of China (22374073), State Key Laboratory of Analytical Chemistry for Life Science (5431ZZXM2204, 5431ZZXM2307) and Supporting by the Program for Outstanding PhD Candidates of Nanjing University.

Conflict of Interests

The authors declare no conflict of interest.

Data Availability Statement

The data that support the findings of this study are available from the corresponding author upon reasonable request.

Keywords: DNA-based biosensors · *In vivo*·miRNA·detection · NIR-II imaging · Signal amplification · Stimulus response

[1] R. Shang, S. Lee, G. Senavirathne, E. C. Lai, *Nat. Rev. Genet.* **2023**, *24*, 816–833.
[2] R. I. Gregory, K. Yan, G. Amuthan, T. Chendrimada, B. Doratotaj, N. Cooch, R. Shiekhattar, *Nature* **2004**, *432*, 235–240.
[3] Y. Lee, C. Ahn, J. Han, H. Choi, J. Kim, J. Yim, *Nature* **2003**, *425*, 415–419.
[4] H. Dong, J. Lei, L. Ding, Y. Wen, H. Ju, X. Zhang, *Chem. Rev.* **2013**, *113*, 6207–6233.
[5] S. M. Hammond, *Adv. Drug Delivery Rev.* **2015**, *87*, 3–14.
[6] A. Pauli, J. L. Rinn, A. F. Schier, *Nat. Rev. Genet.* **2011**, *12*, 136–149.
[7] C. Li, Y. Feng, G. Coukos, L. Zhang, *AAPS J.* **2009**, *11*, 747–757.
[8] T. H. Thai, D. P. Calado, S. Casola, K. M. Ansel, C. Xiao, Y. Xue, A. Murphy, D. Frendewey, D. Valenzuela, J. L. Kutok, M. Schmidt-Supprian, N. Rajewsky, G. Yancopoulos, A. Rao, K. Rajewsky, *Science* **2007**, *316*, 604–608.
[9] a) G. A. Calin, C. M. Croce, *Nat. Rev. Cancer* **2006**, *6*, 857–866; b) S. Asaga, C. Kuo, T. Nguyen, M. Terpenning, A. E. Giuliano, D. S. Hoon, *Clin. Chem.* **2011**, *57*, 84–91.
[10] Y. Wen, J. Han, J. Chen, J. Dong, Y. Xia, J. Liu, Y. Jiang, J. Dai, J. Lu, G. Jin, J. Han, Q. Wei, H. Shen, B. Sun, Z. Hu, *Int. J. Cancer* **2015**, *137*, 1679–1690.
[11] H. Wang, R. Peng, J. Wang, Z. Qin, L. Xue, *Clin. Epigenet.* **2018**, *10*, 59.
[12] M. A. Cortez, C. B. Ramos, J. Ferdin, G. L. Berestein, A. K. Sood, G. A. Calin, *Nat. Rev. Clin. Oncol.* **2011**, *8*, 467–477.
[13] Y. Wang, Q. Yang, Z. Gao, H. Dong, *Biosens. Bioelectron.* **2022**, *212*, 114423.
[14] T. Jet, G. Gines, Y. Rondelez, V. Taly, *Chem. Soc. Rev.* **2021**, *50*, 4141–4161.
[15] S. Cai, T. Pataillot-Meakin, A. Shibakawa, R. Ren, C. L. Bevan, S. Ladame, A. P. Ivanov, J. B. Edel, *Nat. Commun.* **2021**, *12*, 3515.
[16] S. Roush, F. J. Slack, *Trends Cell Biol.* **2008**, *18*, 505–516.
[17] Y. Wang, Y. Xiong, K. Shi, C. Y. Effah, L. Song, L. He, J. Liu, *Chem. Soc. Rev.* **2024**, *53*, 4020–4044.
[18] P. Amero, G. L. R. Lokesh, R. R. Chaudhari, R. Cardenas-Zuniga, T. Schubert, Y. M. Attia, E. Montalvo-Gonzalez, A. M. Elsayed, C. Ivan, Z. Wang, V. Cristini, V. D. Franciscis, S. Zhang, D. E. Volk, R. Mitra, C. Rodriguez-Aguayo, A. K. Sood, G. Lopez-Berestein, *J. Am. Chem. Soc.* **2021**, *143*, 7655–7670.
[19] a) J. I. Cutler, E. Auyeung, C. A. Mirkin, *J. Am. Chem. Soc.* **2012**, *134*, 1376–1391; b) M. Deng, M. Li, X. Mao, F. Li, X. Zuo, *Chem. Res. Chin. Univ.* **2020**, *36*, 185–193.
[20] a) C. Xue, S. Hu, Z. Gao, L. Wang, M. Luo, X. Yu, B. Li, Z. Shen, Z. Wu, *Nat. Commun.* **2021**, *12*, 2928; b) W. Wang, M. Lin, Y. Chen, W. Wang, J. Lv, Y. Chen, H. Yin, Z. Shen, Z. Wu, *Anal. Chem.* **2024**, *96*, 1488–1497.
[21] N. C. Seeman, *Nature* **2003**, *421*, 427–431.
[22] a) J. Liu, Z. Cao, Y. Lu, *Chem. Rev.* **2009**, *109*, 1948–1998; b) A. E. Rangel, A. A. Hariri, M. Eisenstein, H. T. Soh, *Adv. Mater.* **2020**, *32*, 2003704.
[23] N. Li, F. Shen, Z. Cai, W. Pan, Y. Yin, X. Deng, X. Zhang, J. O. A. Machuki, Y. Yu, D. Yang, Y. Yang, M. Guan, F. Gao, *Small* **2020**, *16*, 2005511.
[24] L. Zheng, Q. Li, Y. Wu, L. Su, W. Du, J. Song, L. Chen, H. Yang, *Chem. Sci.* **2023**, *14*, 13860–13869.
[25] G. Bao, J. Sun, H. Zheng, J. Hou, J. Huang, J. Wei, Y. Fu, J. Qiu, X. Zou, B. Xiang, J. Cai, *Front. Oncol.* **2021**, *11*, 747305.
[26] X. Huang, J. Song, B. C. Yung, X. Huang, Y. Xiong, X. Chen, *Chem. Soc. Rev.* **2018**, *47*, 2873–2920.
[27] J. Zhao, Z. Di, L. Li, *Angew. Chem. Int. Ed.* **2022**, *61*, e202204277.
[28] C. Xing, Q. Lin, X. Gao, T. Cao, J. Chen, J. Liu, Y. Lin, J. Wang, C. Lu, *ACS Appl. Mater. Interfaces* **2022**, *14*, 39866–39872.
[29] J. Wei, H. Wang, Q. Wu, X. Gong, K. Ma, X. Liu, F. Wang, *Angew. Chem. Int. Ed.* **2020**, *59*, 5965–5971.
[30] Y. Shang, Y. Chen, Q. Wang, Y. He, S. He, S. Yu, X. Liu, F. Wang, *Nano Today* **2022**, *45*, 101553.
[31] Z. Zhang, Y. Wang, N. Zhang, S. Zhang, *Chem. Sci.* **2016**, *7*, 4184–4189.
[32] W. Dai, H. Dong, K. Guo, X. Zhang, *Chem. Sci.* **2018**, *9*, 1753–1759.
[33] a) F. Wang, J. Elbaz, C. Teller, I. Willner, *Angew. Chem. Int. Ed.* **2010**, *50*, 295–299; b) C. W. Brown, M. R. Lakin, E. K. Horwitz, M. L. Fanning, H. E. West, D. Stefanovic, S. W. Graves, *Angew. Chem. Int. Ed.* **2014**, *53*, 7183–7187.
[34] a) G. Feng, X. Luo, X. Lu, S. Xie, L. Deng, W. Kang, F. He, J. Zhang, C. Lei, B. Lin, Y. Huang, Z. Nie, S. Yao, *Angew. Chem. Int. Ed.* **2019**, *58*, 6590–6594; b) W. Zhou, R. Saran, J. Liu, *Chem. Rev.* **2017**, *117*, 8272–8325.
[35] D. Yi, J. Zhao, L. Li, *Angew. Chem. Int. Ed.* **2021**, *60*, 6300–6304.
[36] H. Peng, X. Li, H. Zhang, X. C. Le, *Nat. Commun.* **2017**, *8*, 14378.
[37] B. Li, Y. Lu, X. Huang, Y. Ning, Q. Shi, J. Liu, B. Liu, *Small* **2023**, *20*, 2305777.
[38] P. Yin, H. M. T. Choi, C. R. Calvert, N. A. Pierce, *Nature* **2008**, *451*, 318–322.
[39] a) Q. Wei, J. Huang, J. Li, J. Wang, X. Yang, J. Liu, K. Wang, *Chem. Sci.* **2018**, *9*, 7802–7808; b) A. P. K. K. Karunanayake Mudiyanselage, Q. Yu, M. A. Leon-Duque, B. Zhao, R. Wu, M. You, *J. Am. Chem. Soc.* **2018**, *140*, 8739–8745.
[40] B. Li, Y. Liu, Y. Liu, T. Tian, B. Yang, X. Huang, J. Liu, B. Liu, *ACS Nano* **2020**, *14*, 8116–8125.
[41] Z. Fan, B. Li, Y. Wang, X. Huang, B. Li, S. Wang, Y. Liu, Y. Liu, B. Liu, *Chem. Sci.* **2022**, *13*, 11197–11204.
[42] R. M. Dirks, N. A. Pierce, *Proc. Natl. Acad. Sci. USA* **2004**, *101*, 15275–15278.
[43] Z. Cheglakov, T. M. Cronin, C. He, Y. Weizmann, *J. Am. Chem. Soc.* **2015**, *137*, 6116–6119.
[44] H. Wu, T. Chen, X. Wang, Y. Ke, J. Jiang, *Chem. Sci.* **2020**, *11*, 62–69.
[45] a) Z. Wu, G. Liu, X. Yang, J. Jiang, *J. Am. Chem. Soc.* **2015**, *137*, 6829–6836; b) L. Li, J. Feng, H. Liu, Q. Li, L. Tong, B. Tang, *Chem. Sci.* **2016**, *7*, 1940–1945.
[46] a) C. M. Agapakis, P. M. Boyle, P. Silver, *Nat. Chem. Biol.* **2012**, *8*, 527–535; b) J. W. Lee, D. Na, J. M. Park, J. Lee, S. Choi, S. Y. Lee, *Nat. Chem. Biol.* **2012**, *8*, 536–546.
[47] S. Zhao, S. Zhang, H. Hu, Y. Cheng, K. Zou, J. Song, J. Deng, L. Li, X. B. Zhang, G. Ke, J. Sun, *Angew. Chem. Int. Ed.* **2023**, *62*, e202303121.
[48] Y. Yin, W. Xie, M. Xiong, Y. Gao, Q. Liu, D. Han, G. Ke, X. B. Zhang, *Angew. Chem. Int. Ed.* **2023**, *62*, e202309837.
[49] K. Ren, Y. Xu, Y. Liu, M. Yang, H. Ju, *ACS Nano* **2017**, *12*, 263–271.
[50] Y. Wang, Y. Li, Y. Zhang, K. Ren, H. Ju, Y. Liu, *Sci. China Chem.* **2020**, *63*, 731–740.
[51] Y. Zhang, W. Chen, Y. Zhang, X. Zhang, Y. Liu, H. Ju, *Angew. Chem. Int. Ed.* **2020**, *59*, 21454–21459.
[52] X. Zhu, B. Qu, Z. Ying, J. Liu, Z. Wu, R. Yu, J. Jiang, *Anal. Chem.* **2020**, *92*, 15953–15958.
[53] a) L. Qiu, C. Wu, M. You, D. Han, T. Chen, G. Zhu, J. Jiang, R. Yu, W. Tan, *J. Am. Chem. Soc.* **2013**, *135*, 12952–12955; b) C. Xue, S. X. Zhang, C. H. Ouyang, D. Chang, B. J. Salena, Y. Li, Z. S. Wu, *Angew. Chem. Int. Ed.* **2018**, *57*, 9739–9743.
[54] J. Hemphill, A. Deiters, *J. Am. Chem. Soc.* **2013**, *135*, 10512–10518.
[55] K. Hwang, P. Wu, T. Kim, L. Lei, S. Tian, Y. Wang, Y. Lu, *Angew. Chem. Int. Ed.* **2014**, *53*, 13798–13802.
[56] J. Zhao, J. Gao, W. Xue, Z. Di, H. Xing, Y. Lu, L. Li, *J. Am. Chem. Soc.* **2018**, *140*, 578–581.

[57] J. Zhao, H. Chu, Y. Zhao, Y. Lu, L. Li, *J. Am. Chem. Soc.* **2019**, *141*, 7056–7062.
[58] Y. Zhang, Y. Zhang, X. Zhang, Y. Li, Y. He, Y. Liu, H. Ju, *Chem. Sci.* **2020**, *11*, 6289–6296.
[59] Y. Shao, J. Zhao, J. Yuan, Y. Zhao, L. Li, *Angew. Chem. Int. Ed.* **2021**, *60*, 8923–8931.
[60] T. Chen, Q. Wu, S. Cao, Q. Zhang, A. Isak, D. Mao, C. Lu, X. Fu, C. Feng, Q. Pan, X. Zhu, *Chem. Eng. J.* **2022**, *430*, 132887.
[61] F. Chen, Q. Lu, L. Huang, B. Liu, M. Liu, Y. Zhang, J. Liu, *Angew. Chem. Int. Ed.* **2021**, *60*, 5453–5458.
[62] M. Ye, Y. Kong, C. Zhang, Y. Lv, S. Cheng, D. Hou, Y. Xian, *ACS Nano* **2021**, *15*, 14253–14262.
[63] X. Chai, Z. Fan, M. Yu, J. Zhao, L. Li, *Nano Lett.* **2021**, *21*, 10047–10053.
[64] a) Z. Xiang, J. Zhao, D. Yi, Z. Di, L. Li, *Angew. Chem. Int. Ed.* **2021**, *60*, 22659–22663; b) L. Li, H. Chen, X. Wen, S. Li, M. Yang, Q. Guo, K. Wang, *CCS* **2023**, *5*, 2403–2414.
[65] a) B. Turk, *Nat. Rev. Drug Discovery* **2006**, *5*, 785–799; b) K. Kessenbrock, V. Plaks, Z. Werb, *Cell* **2010**, *141*, 52–67.
[66] Q. Liu, Y. Huang, Z. Li, L. Li, Y. Zhao, M. Li, *Angew. Chem. Int. Ed.* **2022**, *61*, e202214230.
[67] Y. Zhang, W. Chen, Y. Fang, X. Zhang, Y. Liu, H. Ju, *J. Am. Chem. Soc.* **2021**, *143*, 15233–15242.
[68] a) H. Wang, Y. He, J. Wei, H. Wang, K. Ma, Y. Zhou, X. Liu, X. Zhou, F. Wang, *Angew. Chem. Int. Ed.* **2022**, *61*, e202115489; b) S. He, S. Yu, R. Li, Y. Chen, Q. Wang, Y. He, X. Liu, F. Wang, *Angew. Chem. Int. Ed.* **2022**, *61*, e202206529.
[69] C. Li, G. Chen, Y. Zhang, F. Wu, Q. Wang, *J. Am. Chem. Soc.* **2020**, *142*, 14789–14804.
[70] a) W. Zheng, P. Huang, D. Tu, E. Ma, H. Zhu, X. Chen, *Chem. Soc. Rev.* **2015**, *44*, 1379–1415; b) X. Wang, R. R. Valiev, T. Y. Ohulchanskyy, H. Agren, C. Yang, G. Chen, *Chem. Soc. Rev.* **2017**, *46*, 4150.
[71] C. Wang, Y. Xie, X. Song, Z. Chao, K. Wu, Y. Fang, H. Zhao, H. Ju, Y. Liu, *Angew. Chem. Int. Ed.* **2023**, *62*, e202312665.
[72] H. Chen, M. Su, Y. Lei, Z. Ye, Z. Chen, P. Ma, R. Yuan, Y. Zhuo, C. Yang, W. Liang, *J. Am. Chem. Soc.* **2023**, *145*, 12812–12822.
[73] Z. Wang, S. Xie, L. Wu, F. Chen, L. Qiu, W. Tan, *Nano Lett.* **2022**, *22*, 7853–7859.
[74] a) J. Zhao, Z. Li, Y. Shao, W. Hu, L. Li, *Angew. Chem. Int. Ed.* **2021**, *60*, 17937–17941; b) W. Wei, H. Lu, W. Dai, X. Zheng, H. Dong, *ACS Nano* **2022**, *16*, 20329–20339.

Manuscript received: July 6, 2024
Accepted manuscript online: August 15, 2024
Version of record online: ■■, ■■

CONCEPT

This concept review summarizes signal amplification strategies including DNAzyme catalytic reaction, hybrid chain reaction (HCR), catalytic hairpin assembly (CHA) to enhance detection signal of lowly expressed miRNAs; external stimuli and internal stimuli to prevent nonspecific activation; and the development of NIR-II fluorescent probes for in vivo miRNA imaging and indicated current challenges for in vivo miRNA imaging.

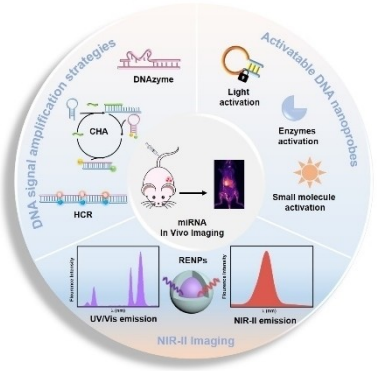

*C. Wang, X. Song, J. Shen, Y. Xie, H. Ju, Y. Liu**

1 – 13

Recent Advances in DNA-Based Nanoprobes for *In vivo* MiRNA Imaging